Timing of the first drainage of the Baltic Ice Lake synchronous with the onset of Greenland Stadial 1

Article

Accepted Version

Timing of the first drainage of the Baltic Ice Lake synchronous with the onset of Greenland Stadial 1

FRANCESCO MUSCHITIELLO, JAMES M. LEA, SARAH L. GREENWOOD, FAEZEH M. NICK, LARS BRUNNBERG, ALISON MACLEOD AND BARBARA WOHLFARTH

Muschitiello, F., Lea, J. M, Greenwood, S. L., Nick, F. M., Brunnberg, L., MacLeod, A., & Wohlfarth, B.: Timing of the first drainage of the Baltic Ice Lake synchronous with the onset of Greenland Stadial 1

Glacial varves can give significant insights into recession and melting rates of decaying ice sheets. Moreover, varve chronologies can provide an independent means of comparison to other annually resolved climatic archives, which ultimately help to assess the timing and response of an ice sheet to changes across rapid climate transitions. Here we report a composite 1257-year long varve chronology from south-eastern Sweden spanning the regional late Allerød-late Younger Dryas pollen zone. The chronology was correlated to the Greenland Ice Core Chronology 2005 using the time-synchronous Vedde Ash volcanic marker, which can be found in both successions. For the first time, this enables secure placement of the Lateglacial Swedish varve chronology in absolute time. Geochemical analysis from new varve successions indicate a marked change in sedimentation regime accompanied by an interruption of ice-rafted debris deposition synchronous with the onset of Greenland Stadial 1 (GS-1; 12 846 years before 1950 AD). With the support of a simple ice flow/calving model, we suggest that slowdown of sediment transfer can be explained by ice-sheet margin stabilisation/advance in response to a significant drop of the Baltic Ice Lake level. A reassessment of chronological evidence from central-western and southern Sweden further supports the hypothesis of synchronicity between the first (penultimate) catastrophic drainage of the Baltic Ice Lake and the start of GS-1 in Greenland ice cores. Our results may therefore provide the first chronologically robust evidence linking continental meltwater forcing to rapid atmosphere-ocean circulation changes in the North Atlantic.

Francesco Muschitiello (Francesco.muschitiello@geo.su.se), Sarah L. Greenwood and Barbara Wohlfarth, Department of Geological Sciences and Bolin Centre for Climate

Research, Stockholm University, SE-10691, Stockholm, Sweden; James M. Lea and Lars Brunnberg, Department of Physical Geography and Bolin Centre for Climate Research, Stockholm University, SE-10691, Stockholm, Sweden; Faezeh M. Nick, Department of Geology, University Centre in Svalbard (UNIS), PO Box 156, NO-9171 Longyearbyen, Norway, Centre for Ice and Climate, Niels Bohr Institute, University of Copenhagen, 2100 Copenhagen, Denmark; Alison MacLeod, Department of Geography, Royal Holloway University of London, Egham, Surrey TW20 0EX, UK.

Understanding the timing and interplay between past ice-sheet dynamics and abrupt climate change can be significantly enhanced where suitable highly resolved and independently dated palaeoenvironmental archives are available. Glacial varves are such a proxy, providing an indirect record for ice-marginal dynamics at potentially annual or sub-annual resolution. Furthermore, these records can provide lengthy and continuous chronologies, which can be directly compared to other climate archives. In turn, this allows the examination of potential couplings between changing regional ice-sheet behaviour and climate change.

The Swedish glacial varve chronology or 'Swedish Time Scale' (STS) provides a reconstruction preserving information regarding the dynamics and the melting of the Fennoscandian Ice Sheet (FIS). It is therefore an ideal data set to investigate ice sheet dynamics and sensitivity in response to climate change. The STS is based on visual cross-correlation of more than 1000 ice-proximal clastic varve-thickness successions, which reflect the seasonal sediment input associated with the deglaciation of Sweden (De Geer 1912, 1940). These clastic varves, with their distinct silt dominated summer and clay dominated winter layers were deposited in the ice-dammed Baltic basin, the

54 Baltic Ice Lake (BIL), and can today be found along the Baltic Sea coast and in the Baltic
55 Sea (Strömberg 1985; Cato 1987; Björck *et al.* 1992; Brunnberg 1995; Wohlfarth *et al.*
56 1994, 1995). The younger part of the STS is made up of postglacial delta sediments,
57 which were and still are deposited in the estuary of River Ångermanälven in northern
58 Sweden (Cato 1985, 1987, 1998; Wohlfarth *et al.* 1997). However, a putative gap of
59 700-900 varve years during the early and/or mid Holocene (Wohlfarth 1996;
60 Wohlfarth *et al.* 1997; Andrén *et al.* 1999), as well as difficulties in correlating varve
61 diagrams from Blekinge in southernmost Sweden to those of south-eastern Sweden
62 (Wohlfarth & Possnert 2000) has so far posed a challenge to establishing an absolute
63 and continuous varve chronology from present back to >14 000 varve years. Given
64 the chronological uncertainties due to missing varves, each regional varve chronology
65 thus stands on its own (Wohlfarth & Possnert, 2000).

66 The Lateglacial clay-varve diagrams from south-eastern Sweden (northern
67 Småland and Östergötland) (Kristiansson 1986; Brunnberg 1995; Wohlfarth *et al.*
68 1993, 1994, 1995, 1998), spanning the later part of the regional Allerød pollen zone
69 (AL) and the early part of the regional Younger Dryas pollen zone (YD), constitute one
70 of the most valuable portions of the STS. This Lateglacial varve chronology (LGC) is
71 built by visual cross-correlations and corroborated by statistical analysis (Holmquist &
72 Wohlfarth 1998), but is at present only tentatively linked to a calendar-year time scale
73 by means of ^{14}C dating (Goslar *et al.* 1999; Wohlfarth & Possnert, 2000).

74 The recent finding of the Vedde Ash in a glacial varve succession from the same
75 region (MacLeod *et al.* 2014) now offers an excellent opportunity to secure the
76 floating LGC chronology to an absolute time scale, and more importantly, to correlate
77 this section of the STS to the Greenland ice-core chronology. Through the temporal

accuracy this affords, the resulting correlation can therefore reveal crucial information regarding the temporal coupling between Fennoscandian ice-sheet dynamics and rapid climate change.

Here we reassess, update and extend the 806-year long LGC from south-eastern Sweden (Wohlfarth *et al.* 1998), and link for the first time the FIS recession to the Greenland ice-core time scale. The existing chronology has, moreover, been complemented by new geochemical data and corroborated by idealised numerical modelling of ice dynamics. These help to cast light on the changes that occurred in the BIL terminating sector of the FIS around the onset of the YD. Our results highlight a possible linkage between changes in ice sheet behaviour associated with the drainage of the BIL and abrupt changes in atmosphere-ocean circulation in the North Atlantic domain.

Study area and methods

Study area

The LGC derives from sites located along the eastern edge of the southern Swedish Uplands. The terrain reaches >330 m elevation above present-day sea level in the south and west of our area of interest, sloping eastwards and northwards towards the Baltic Sea (Fig. 1B, C). The FIS retreated broadly NW-wards across this region. Clay-varve chronologies have hitherto been the primary source of information regarding the pattern and timing of ice retreat (cf. Lundqvist & Wohlfarth 2001). An absence of moraines across south-eastern Sweden suggests unpunctuated retreat, an exception being the Vimmerby moraine that cuts across the south of our study area (Fig. 1C). Fed by fairly uniform SE-ward flow, this ice-margin position has been constrained by

cosmogenic nuclide dating to 14 600-14 400 cal. years ago (Johnsen *et al.* 2009; Anjar *et al.* 2014). There is no further evidence of a sustained ice-margin position until the Middle Swedish End Moraine Zone (MSEMZ), a broad (~10-20 km) zone stretching from Lake Vättern ENE across the Östergötland lowlands. Associated with the YD, the MSEMZ comprises moraines, deltas and glacio-tectonised successions linked with ice margin oscillations and an extremely slow rate of retreat (Kristiansson 1986; Lundqvist 1987).

Glacial lakes were impounded across south-eastern Sweden in front of the retreating ice margin, both localised and linked to the much larger BIL, which was up-dammed in the Baltic Sea Basin. The BIL was maintained by the ice dam across central-southern Sweden and the southern Swedish uplands and the high threshold level in Öresund; not until the ice margin retreated past Mt. Billingen could any drainage occur (Björck 1995). A major (25 m lake-level drop) and rapid (1-2 years) drainage of the BIL, and consequent opening to marine waters (Yoldia Sea stage), occurred at the end of the YD when the Billingen ice dam was released (Björck & Digerfeldt 1984; Björck 1995; Johnson *et al.* 2013). An earlier drainage is hypothesised to have occurred at the late AL-YD transition (Björck 1995; Bennike & Jensen 2013), but its magnitude and dynamics are less well-constrained. Palaeo-shorelines of the BIL are evident along the east and south coast of Sweden, rising to the north as a consequence of post-glacial (and ongoing) glacio-isostatic rebound (see Fig. 1).

AL-age glacial varved-clay successions from sites close to the former highest shoreline of the BIL had earlier been investigated in the provinces of Småland and Östergötland (Kristiansson 1986; Wohlfarth *et al.* 1995, 1998) (Fig. 1). Most of the varve thickness diagrams were obtained in a region that formed an archipelago-like

126 landscape in the western part of the large BIL (Wohlfarth *et al.* 1998). The glacial
127 varves were thus deposited in fairly shallow waters (between ~5 and 70 m) and mostly
128 within a large fjord complex (Fig. 1). Owing to isostatic uplift of the newly deglaciated
129 areas, progressive shallowing of the depositional basins along the coast and successive
130 isolation resulted in a cessation of varve deposition and replacement by homogeneous
131 clay and organic lacustrine sediments. The recently published varve chronology from
132 Gropviken (MacLeod *et al.* 2014) and the varve chronology from Sandfjärden (this
133 study), ~50 km farther to the east, derive from sites that were located directly south
134 of the YD ice margin (Fig. 1) and at a former BIL water depth of approximately 100 m
135 (Brunnberg 1995).
136
137 *Varve and ^{14}C chronologies*
138 The original master chronology for Småland/Östergötland (the LGC) is a composite
139 chronology of 806 varve years (Wohlfarth *et al.* 1998; Wohlfarth & Possnert 2000),
140 which is based on the visual linking of common and distinct sedimentological features
141 in 55 varve diagrams (Figs. 1, 2). These correlations are corroborated by cross-
142 correlation analysis (Holmquist & Wohlfarth 1998). The chronology from Gropviken is
143 a 710 varve-year long record, which contains the Vedde Ash isochrone (MacLeod *et*
144 *al.* 2014). The chronology from Sandfjärden is a 623 varve-year long record (Fig. 1C).
145 AMS radiocarbon measurements that had been published earlier for selected
146 sites of the LGC (Wohlfarth *et al.* 1998; Wohlfarth & Possnert 2000) are here used to
147 verify the internal consistency of the new composite varve chronology (Table 1). To
148 provide the most reliable ^{14}C-based chronology, we selected only those ^{14}C
149 measurements that had been made on terrestrial plant macrofossil remains and we

disregarded dates that were associated with unidentified and reworked plant material or had analytical errors of >250 years (Wohlfarth *et al.* 1998; Wohlfarth & Possnert 2000).

Based on Bayesian wiggle-match modelling using OxCal4.2 (Bronk Ramsey 2010), these ^{14}C dates were used to find the most likely possible placement of the LGC on the IntCal13 radiocarbon calibration curve (Reimer *et al.* 2013). Outlying dates were detected by the software applying the 'Outlier Analysis' and discarded until a satisfactory and coherent age model was generated as defined by a high model agreement with values higher than a threshold of 60% (Bronk Ramsey 2009).

New cores: fieldwork, dating and elemental analyses

A new sediment succession from Lake Gummetorpasjön, which was previously investigated by Wohlfarth *et al.* (1998), was cored in March 2015 (Fig. 1), with the purpose of performing geochemical analysis. Parallel sediment cores were collected using a 1-m long Russian corer with diameters of 10 and 7.5 cm, obtaining 50 cm overlapping sections.

Correlation to the previously established LGC chronology (Wohlfarth *et al.* 1998) was carried out employing three distinct colour and varve thickness changes that were identified by Wohlfarth *et al.* (1998). The marker layers, which occur 115 and 108 varve years apart from each other, are present in the majority of the varve diagrams that compose the LGC, including Gummetorpajön (see discussion below). This allowed the new XRF profiles to be placed unequivocally within the existing chronology.

The new Gummetorpasjön sediment cores were scanned at the Department of Geological Sciences at Stockholm University using an ITRAX XRF Core Scanner from

Cox Analytical System (Gothenburg, Sweden) to detect chemical changes and signals relating to summer and winter layers. Radiographic images were generated using a Mo tube set at 55 kV and 50 mA with a step size of 200 µm and a dwell time of 400 ms. XRF data were acquired using a Mo tube set at 30 kV and 50 mA with a step size of 200 µm and a dwell time of 30 s. Based on XRF counting statistics of the new Gummetorpasjön clay-varve record, reliable data were obtained for 21 elements with signals well above the instrumental noise threshold making it unnecessary to normalize the peak area data to the scattering. Relative changes in peak areas of elemental data were therefore used to construct ratio profiles from selected elements, i.e. Zr, Rb, Fe and Ca. Elemental XRF core scanning profiles were used as indicators of changes in sediment transfer rates and grain size mediated by local ice-mass turnover within the fjord system.

Results and discussion

Reconstruction of the new Lateglacial varve chronology

To anchor the LGC to the chronology of Gropviken, which contains the Vedde Ash, we approached the alignment systematically (see below), initially adopting Kristiansson's (1986) original time scale.

The first step taken for correlating the Gropviken varve thickness diagram and each one of the diagrams composing the LGC was to search for statistically significant cross-correlations between the successions, though this proved unsuccessful due to substantial differences in varve thicknesses.

We therefore introduced an additional alignment step by bridging Gropviken's chronology and the LGC using the Sandfjärden floating varve chronology from the

198 northern sector of Östergötland (Fig. 1C). The cross-correlation of varve thickness
199 diagrams from Gropviken and Sandfjärden provided a statistically significant match (r
200 = 0.61, signal-to-noise ratio z = 7.7, p = 0.99) that enabled us to extend the varve
201 chronology to the northern sector of Östergötland (Fig. 3).

202 In a next step we linked the Sandfjärden chronology to the LGC. However, cross-
203 correlations alone could not directly link the two chronologies together. The
204 chronologies were therefore aligned via identification of three common markers, i.e.
205 two colour changes at local varve years 2060 and 2169, and a characteristic thick varve
206 horizon at local varve year 2060 (Fig. 3). This technique (e.g. Palmer *et al.* 2010)
207 provided satisfactorily fits between the successions.

208 To provide an independent test of the alignment between the LGC and
209 Gropviken's chronology, we employed an independent ^{14}C dating method (Fig. 4). The
210 LGC is supported by AMS radiocarbon measurements (Wohlfarth *et al.* 1998;
211 Wohlfarth & Possnert 2000), whereas the Vedde Ash has been precisely radiocarbon
212 dated in lake sediment records from western Norway (Lohne *et al.* 2013). The LGC was
213 anchored to the IntCal13 radiocarbon calibration curve using a Bayesian wiggle-
214 matching model based on eight radiocarbon dates. Using the calibrated age of the
215 Vedde Ash and the most likely placement of the LGC on the IntCal13 time scale,
216 respectively, we were able to calculate the offset between the chronology of
217 Gropviken and the LGC, and compare the results with the offset previously obtained
218 from the alignment approach. The offsets resulting from the two methods,
219 respectively, strongly agree with each other (-1353 years using the alignment versus -
220 1359 using wiggle-matching; Fig. 4), which indicates that the relative placement
221 between the northern and southern chronologies is coherent and reliable.

222

223 *Age error evaluation of the Lateglacial varve chronology*

224 The excellent correlation among the 55 varve diagrams that compose the original LGC
225 suggests no or minimal counting errors and laterally continuous varve accumulation
226 over this sector of Småland/Östergötland (Wohlfarth *et al.* 1998). An example of such
227 region-wide chronological consistency is demonstrated by the precision of varve
228 counts in relation to the interval spanning the three marker horizons utilized to link
229 the original LGC to Sandfjärden's chronology (<1% difference).

230 The independent ^{14}C dating approach described in section above provides a
231 means to verify the chronological accuracy over a large interval of the LGC,
232 demonstrating that contributions to uncertainty from undetected systematic errors in
233 the varve layer identification process is minimal (Fig. 4). This is also substantiated by
234 the similarity between the inferred varve age and the unmodelled ^{14}C-calibrated curve
235 (Fig. 4). Moreover, the biostratigraphic boundary of the AL-YD transition, which has
236 been identified in the pollen stratigraphy from Gummetorpasjön (Björck 1999),
237 provides an additional chronostratigraphic constraint that confirms the internal
238 consistency of the LGC. Indeed, even considering the low-resolution pollen sampling
239 (Björck 1999), the estimated ^{14}C-calibrated age of this regionally isochronous marker
240 in the varve stratigraphy falls within the 1σ range of the AL-YD pollen zone boundary
241 observed in some of the most robustly constrained radiocarbon-dated regional
242 records (Muschitiello & Wohlfarth 2015).

243 We are confident that an overall uncertainty (entailing precision and accuracy)
244 of ±0.5% (2σ) is an over-conservative estimate for the unified chronology. This is based
245 on, *i*) the general lack of disturbed or suspicious intervals and the good preservation

of the varves in all the LGC profiles (Wohlfarth *et al.* 1998), *ii*) the evenly high correlation among numerous adjacent and distal sites (Wohlfarth *et al.* 1998), and *iii*) the internal chronological consistency determined via independent dating approaches. This is realistic given that the error that accompanies most varve chronologies with well-developed and undisturbed successions displaying little variations between alternate counts does not exceed ±1% (Zolitschka *et al.* 2015).

Synchronization to Greenland Ice-Core Chronology 2005 and varve stratigraphy

Our new LGC extends over 1257±3 varve years (1σ) and covers the interval from the regional late AL pollen zone to the regional late YD pollen zone. The chronology is based on 57 varve-thickness diagrams, which were compiled to form one unified record of mean varve thickness (Fig. 5). The supporting ^{14}C-based age model enables us to secure the new LGC on the IntCal13 time scale. Critically, we are also now able to synchronize the LGC record with the Greenland Ice-Core Chronology 2005 (Rasmussen *et al.* 2006; after converting the b2k age [before the year 2000] into BP [before 1950 AD], hereafter GICC05 years BP) via the Vedde Ash time marker (Fig. 5). This allows us, for the first time, to directly compare the dynamics of the FIS to the Greenland ice-core event stratigraphy.

Although there are numerous distinct events with exceptionally thick varves, Wohlfarth *et al.* (1998) identified only three major events in their varve chronology, that are recurrent in the majority of the varve diagrams. The Events, numbered 1, 2 and 3 (Wohlfarth *et al.* 1998), are characterised by distinct colour changes of the clay varves and based on the correlation to the ice core time scale occurred at 12 847, 12 739 and 12 624 GICC05 years BP, within one varve year. All the events exhibit a marked

drop in varve thickness that lasts for a few decades. The colour change and the drop in varve thickness make Event 1, 2 and 3 different from all the other anomalous varve layers that can be observed in the new LGC.

Events 2 and 3, which are both preceded by an exceptionally thick varve, have been attributed to drainages of ice-dammed lakes located west of the BIL (Wohlfarth *et al.* 1998). These events are present in all varve diagrams except for Skedevi, Räfstad and Kråkedal (sites 17, 20 and 21 in Fig. 1). As such, large areas above the highest shoreline remained covered by stagnant ice and continued to contribute sediment material to the BIL as the ice sheet retreated (Lundqvist & Wohlfarth 2001). However, it remains unclear why a decrease in varve thickness accompanies all of the events. Event 1 in particular, which can be observed in all the varve diagrams covering this interval (Figs. 1, 2), presents the most pronounced decrease in varve thickness of the entire chronology, but is not preceded by a thick varve (Fig. 5). This suggests that the causes of Event 1, which can be traced for more than 25 km eastwards (from Gummetorpasjön to Tynn – Wohlfarth *et al.* 1998), are potentially not just a mere response to a release of high amounts of sediment material into the BIL. Moreover, based on a previously published ice-rafted debris (IRD) record (Wohlfarth *et al.* 1998) that accompanies the LGC (Fig. 5), it is evident that, unlike Events 2 and 3, Event 1 is the only one associated with a long-term interruption (~130 varve years) in IRD deposition.

We note that, after synchronizing the varve record to the Greenland time scale, Event 1 coincides with the transition from Greenland Interstadial 1 to Greenland Stadial 1 (GS-1), which is defined in NGRIP ice cores as an abrupt shift in *d*-excess that took place within 2-3 years (Steffensen *et al.* 2008). The onset of GS-1 is dated to 12

846±69 GICC05 years BP considering 1σ age uncertainty in the GICC05 (i.e. half of the total maximum counting error – MCE; Rasmussen *et al.* 2006) and Event 1 is dated to 12 847±2 GICC05 years BP (accounting for 1σ of the total uncertainty that accompanies the LGC). This places GS-1 and Event 1 at 725±6 years and 726±2 years, respectively, prior to the Vedde Ash in their respective records.

The temporal consistency of Event 1 relative to the start of GS-1 requires further attention. In the following, we focus on the varve stratigraphic boundary identified at 12 847±71 GICC05 years BP by reporting and discussing the results from XRF analyses on Gummetorpasjön's succession in conjunction with output from idealised ice flow model simulations.

Geochemical evidence of depositional changes at the GI-1/GS-1 transition

We use Zr/Rb and Fe/Ca ratios as proxies for grain-size distribution and composition (Fig. 6). Rb, which is common in several minerals, has generally low environmental mobility owing to strong sorption in clay minerals. Conversely, Zr is usually found in medium to coarse silts and is present in heavy minerals. In fine-grained sediments - like in our clay varves, Zr/Rb is thus an ideal proxy for grain size (Dypvik & Harris 2001). Like Rb, Fe absorbs onto clay and has relatively low mobility, whereas Ca can easily be found in plagioclase and calcite in the sand and silt fraction (e.g. Johnson *et al.* 2013). Thus, Fe/Ca can be used here as an additional indicator for grain size.

The XRF data profiles entirely resolve seasonal varves associated with summer and winter accumulation, with summer laminae generally characterised by larger grain sizes as compared to winter laminae (Fig. 6). The XRF stratigraphies consistently show a decrease in grain size 18-19 varve years before Event 1 at 12 847 GICC05 years

318 BP (Fig. 6). At 12 847 GICC05 years BP the ratio values abruptly shift indicating a
319 change towards coarser grain sizes. The shift takes place within one varve year, after
320 which the geochemical parameters indicate that depositional conditions directly enter
321 into a new stable state for a period that lasted 57-58 varve years (Fig. 6).

322 We infer increased sediment supply of fine sediments during the two decades
323 preceding Event 1, followed by a marked slowdown of sediment transfer and increase
324 in grain size at 12847 GICC05 years BP. This is coeval with a distinct drop in varve
325 thickness and disappearance of IRD (Fig. 5). The rapid change in varve thickness and
326 grain size suggest a potential large-scale shift in the lake circulation regime and/or
327 changes to how sediments are supplied to the lake.

328 Stabilisation of the ice sheet's calving margin could achieve the observed
329 changes in IRD delivery. Increased stability can be driven by glacio-isostatic rebound
330 of the crust and commensurate reduction in the proglacial water depth (Gomez *et al.*
331 2010), though its gradual nature cannot explain the abrupt sedimentation changes
332 observed in the LGC records. Rather, we suggest that a rapid fall of the BIL water level,
333 reducing calving margin buoyancy, and therefore calving, acted to abruptly decrease
334 iceberg calving flux from the ice margin.

335 The coupling between a rapid lowering of the BIL and a general decrease in varve
336 thickness together with interruption of IRD deposition has been suggested for the final
337 drainage of the BIL around the YD-Preboreal transition (Andrén *et al.* 1999, 2002). We
338 therefore argue that the evidence in the LGC and in our geochemical records
339 associated with Event 1 represent a late AL drainage of the BIL (Björck 1995). This
340 would be caused by a recession of the southern margin of the FIS beyond the lake

341 outlet. In the following, we explore the implications of this hypothesis by means of
342 simulations from a simple ice flow/calving model.
343
344 *Ice-sheet response to Baltic Ice Lake drainage*
345 A series of experiments simulating a highly idealised glacier calving margin were
346 undertaken using a well-established one-dimensional flow-line numerical model (Nick
347 *et al.* 2010) and applying a simple floatation based calving law (Vieli *et al.* 2001). These
348 were conducted to investigate changes in calving rate and terminus position following
349 a drop in lake level for a flat-bedded ice sheet. These experiments do not seek to
350 directly simulate the ice draining into the BIL, but rather illustrate the potential
351 dynamic response of an ice sheet that experiences a drop in its proglacial lake level.
352 The specifics of the model are discussed in detail elsewhere (e.g. Nick *et al.* 2010), with
353 relevant input parameters shown in Table 2.
354 The model is used to investigate calving and terminus response with respect to
355 three variables: basal roughness, initial bed depth, and size of lake-level drop. Three
356 basal roughness scenarios were tested, chosen to represent a smooth, medium and
357 rough sliding scenarios, with values defined within the range of those used for
358 contemporary Greenland modelling studies (e.g. Nick *et al.* 2013; Lea *et al.* 2014a, b).
359 Three initial bed elevations were also chosen, equivalent to the mean, 25^{th} and 75^{th}
360 percentile values of a transect spanning an estimated pre-YD ice margin, isostatically
361 depressed according to the Ice5G model (Peltier 2004). Finally, three different lake-
362 level drops were simulated (10, 20 and 30 m), based on current estimates of the
363 magnitude of the hypothesized pre-YD BIL drainage (Björck 1995; Bennike & Jensen
364 2013).

Results of highly idealised numerical model experiments investigating calving and terminus behaviour are shown in Fig. 7. These demonstrate that in all cases a drop in lake level would cause both a reduction in calving compared to the pre-drainage iceberg flux and an advance of the ice-calving terminus. However, the magnitude of these changes, ranging from 10% to 45%, is highly dependent on the initial lake depth and size of the lake drop. While changes in calving are broadly unaffected by the basal conditions of the ice stream, Fig. 7 also shows that rougher bed conditions limit how far the glacier calving margin can advance following a lake level drop (though it should be emphasised that these should not be equated to estimates of actual advance distances of FIS following lake drainage).

The results provide evidence that the proportional reduction in calving rates will have been greatest in shallow areas of the BIL. Larger drops in lake level result in greater proportional decreases in calving flux, as is consistent with the floatation calving law employed in the model. However, these larger drops would also increase the range of calving response between shallow and deeper areas of the BIL terminating sectors of FIS.

Model results suggest that the BIL terminating sectors of the FIS will have experienced a decrease in calving flux due to decreased buoyancy (and hence stabilisation) of the ice margin. Although calving rates will have responded almost instantaneously to a drop in lake level, this is likely to only impact IRD frequency (as identified) rather than the deposition of finer grained sediments on a lake-wide scale. By itself, this can only partially explain the observed drop in IRD frequency, though it is worth noting that a thinner calving margin would also produce smaller, and therefore less long-lived icebergs. Faster melting icebergs would therefore decrease

the probability of IRD deposition in ice distal/sheltered parts of the post-drainage BIL. A further consideration is that changes in lake circulation resulting from the drop in BIL may have caused debris-laden icebergs to be diverted elsewhere from the coring sites.

The presence of thinner varves following the drainage suggests that reworking of material from newly exposed areas of the former lake bed did not result in significant sediment supply into the lake basin. We therefore hypothesise that the shift in observed sedimentation rates resulted from a rapid change in the delivery rate of subglacially derived material to the lake. However, further investigation regarding the major sediment sources for the varves would be required for this to be fully substantiated.

The first drainage of the Baltic Ice Lake

During the latter part of the AL, rapid deglaciation of the southern FIS margin near Mt. Billingen - in the south-central Swedish low-land area (Fig. 1B) – is thought to have generated a spillway system that connected the BIL to the sea in the west (e.g. Björck & Möller 1987; Björck 1995; Lundqvist & Wohlfarth 2001). A rapid retreat of the FIS west of the outlet resulted in a 5-10 m lowering of the BIL (Björck 1995) also referred to as the first drainage of the BIL.

Although this drainage hypothesis has long been debated, new reconstructions support the occurrence of a late AL connection between the BIL and the North Atlantic (Swärd *et al.* 2015) and a significant drop of the BIL water level at this time (Bennike & Jensen 2013). Shore displacement curves from Hunneberg, west of Mt. Billingen, provide a detailed framework for the timing of the deglaciation near the outlet and

413 the freshwater connection to the sea (e.g. Björck & Digerfeldt 1982a, b). The published
414 radiocarbon dates associated with the shoreline reconstructions have recently been
415 re-calibrated and combined using a Bayesian framework (Muschitiello *et al.* in press).
416 The radiocarbon dates indicate lake isolations from the sea near 11 000 ^{14}C years BP
417 (~□□□□□□□□□□□□□□□□□□.□□ea□s□□□), a result of the deglaciation north of Mt. Billingen
418 (Björck & Digerfeldt 1982a, b). Therefore, the dates provide a chronological estimate
419 of the opening of the outlet at Mt. Billingen.

420 The combined age probability of the radiocarbon dates associated with lake
421 isolations has been compared to the age estimate of Event 1 derived from the
422 radiocarbon-based age model that underpins the LGC (Fig. 8). The two independent
423 age estimates, based on wiggle-matching and on radiocarbon calibration, are
424 remarkably similar (12867±66 cal. years BP for the opening of the outlet at Mt.
425 Billingen versus 12876±22 cal. years BP for Event 1). The good chronological
426 correspondence supports our hypothesis of late AL drainage of the BIL synchronous
427 with the start of GS-1 in the Greenland ice core chronology. Furthermore, the
428 observed offset of 30±22 years (1σ) between the GICC05 and the IntCal13 time scales
429 at the transition into GS-1 (Fig. 8) compares well with an offset of 40±30 years (1σ)
430 estimated with other independent methods of time-scale synchronization (Muscheler
431 *et al.* 2014).

432 We suggest that Event 1 can provide a precise chronological tie point that can
433 facilitate regional correlations for future varve reconstructions. In addition, this
434 stratigraphic marker - and more broadly any direct evidence of the first drainage of
435 the BIL - can potentially be used as an isochronous horizon to link records from the

436 Baltic Sea, southern Sweden and the eastern sector of the North Sea downstream of
437 the drainage route.
438
439 *Palaeoclimatic implications*
440 The abrupt shift in *d*-excess values that marks the onset of GS-1 in the NGRIP ice cores
441 (Steffensen *et al.* 2008) can be ascribed to a large southward shift of the marine
442 moisture source for Greenland precipitation (Pfahl & Sodemann 2014) driven by a
443 southward displacement of the North Atlantic westerly winds (Muschitiello *et al.* in
444 press). It has been hypothesised that such an abrupt southward diversion of the
445 westerly winds could have been triggered by a comparably abrupt westward
446 expansion of sea ice in the Nordic Seas (Muschitiello *et al.* in press). However, the
447 driving forces behind this putative swift growth of regional sea ice are still not entirely
448 discerned.
449 A catastrophic drainage of freshwater from the BIL can provide a plausible
450 explanation for a westward migration of sea ice in the Nordic Seas, and especially for
451 its abruptness, thereby providing a physical mechanism and timing for the start of GS-
452 1. We hypothesize that a powerful surge of Baltic-sourced freshwater routed north
453 along the coast of the Norwegian Sea could have increased sea-ice production and
454 moved, to some extent, sea ice off the shelf area towards the open ocean or
455 recirculated ice in the Nordic Seas. Thus, the excess sea ice was displaced westwards
456 beyond the limits expected from local climatological growth conditions and ultimately
457 exported to the subpolar North Atlantic. This phenomenon could have induced the
458 atmospheric circulation to cross thresholds beyond which the seasonal distribution of
459 sea ice in the Nordic Seas became significantly altered, instigating a widespread

460 expansion of sea ice in the North Atlantic. Nonetheless, this explanation remains
461 speculative until more detailed climate modelling studies surrounding the
462 atmosphere-ocean response to Fennoscandian meltwater outlets can be undertaken.
463
464 **Conclusions**
465 In this study we have revaluated and extended a Swedish Lateglacial varve chronology,
466 which now forms a continuous 1257-year long record spanning the period from the
467 regional late AL to the late YD pollen zone. The chronology has been secured to the
468 GICC05 and IntCal13 absolute time scales. Correlation to the Greenland ice-core
469 framework allows us, for the first time, to compare the melting history of the FIS with
470 ice-core climate events.
471 By using geochemical analyses and ice-flow modelling simulations, we suggest
472 that in the late AL a major drop of the BIL water level associated with the first drainage
473 of the BIL occurred. The drainage took place synchronously with the start of GS-1 and
474 specifically 726±2 years prior to the deposition of the Vedde Ash as compared to
475 725±6 years observed in ice-core records. The drainage event would provide a
476 plausible physical explanation for the timing and sign of hydroclimatic shifts observed
477 in the Greenland records, while the related stratigraphic marker can serve as an
478 important chronological tie-point for future regional correlation of proxy records.
479 We hope that this study will inspire future water-hosing and eddy-resolving
480 ocean model simulations that can help to shed light on the forcing mechanisms behind
481 the rapid climate changes that took place at the inception of Greenland Stadial 1 in
482 the North Atlantic region.
483

Acknowledgements. - We are kindly grateful to P. Saarikoski for assistance during fieldwork and M. Kylander for help with XRF core scanning. We are also grateful to M.D. Johnson and an anonymous reviewer for helpful comments on an earlier version of the manuscript. The contribution of JL was supported by FORMAS grant 214-2013-1600 (PI: Nina Kirchner, Stockholm University). This work is a contribution to the INTIMATE project.

References

Andrén, T., Björck, J. & Johnsen, S. 1999: Correlation of Swedish glacial varves with the Greenland (GRIP) oxygen isotope record. *Journal of Quaternary Science 14*, 361–371.

Andrén, T., Lindeberg, G. & Andrén, E. 2002: Evidence of the final drainage of the Baltic Ice Lake and the brackish phase of the Yoldia Sea in glacial varves from the Baltic Sea. *Boreas 31*, 226–238.

Anjar, J., Larsen, N.K., Håkansson, L., Möller, P., Linge, H., Fabel, D. & Xu, S. 2014: A ^{10}Be-based reconstruction of the last deglaciation in southern Sweden. *Boreas 43*, 132-148.

Bennike, O. & Jensen, J.B. 2013: A Baltic Ice Lake lowstand of latest Allerød age in the Arkona Basin, southern Baltic Sea. *Geolological Survey of Denmark and Greenland Bulletin 28*, 17–20.

Björck, S. 1979: Late Weichselian stratigraphy of Blekinge, SE Sweden, and water level changes in the Baltic Ice Lake. *LUNDQUA Thesis 7*, 248 pp.

Björck, J. 1999. The Allerød-Younger Dryas pollen zone boundary in an 800-year varve chronology from southeastern Sweden. *GFF 121*, 287–292.

Björck, S., 1995: A review of the history of the Baltic Sea, 13.0-8.0 ka BP. *Quaternary International 27*, 19–40.

Björck, S. Digerfeldt, G., 1982a: New 14C dates from Hunneberg supporting the revised deglaciation chronology of the Middle Swedish end moraine zone. *GFF 103*, 395–404.

Björck, S. Digerfeldt, G., 1982b: Late Weichselian shore displacement at Hunneberg, southern Sweden, indicating complex uplift. *GFF 104*, 131–155.

515 Björck, S. & Digerfeldt, G. 1984: Climatic changes at Pleistocene/Holocene boundary
516 in the Middle Swedish End Moraine Zone, mainly inferred from stratigraphic
517 indications. In Mörner, N.A., Karlén, W. (eds): *Climatic Changes on a Yearly to*
518 *Millennial Basis*. Reidel Publishing Co., Dordrecht, pp37-56.
519
520 Björck, S. & Möller, P. 1987: Late Weichselian environmental history in southeastern
521 Sweden during the deglaciation of the Scandinavian ice sheet. *Quaternary*
522 *Research 28*, 1–37.

523 Björck, S., Cato, I., Brunnberg, L. & Strömberg, B. 1992: The clay-varve based Swedish
524 Time Scale and its relation to the Late Weichselian radiocarbon chronology. *In*
525 *The Last Deglaciation: Absolute and Radiocarbon Chronologies*, 25–44. Springer,
526 Berlin.

527 Bronk Ramsey, C. 2009: Bayesian analysis of radiocarbon dates. *Radiocarbon 51*, 337–
528 360.

529 Bronk Ramsey, C. 2010: OxCal Program, v. 4.1.7, Radiocarbon accelerator unit,
530 University of Oxford, UK.

531 Brunnberg, L. 1995: Clay-varve chronology and deglaciation during the Younger Dryas
532 and Preboreal in the easternmost part of the Middle Swedish Ice Marginal Zone.
533 *Quaternaria Series A* 2, 1-95.

534 Cato, I. 1985: The definitive connection of the Swedish geochronological time scale
535 with the present, and the new date of the zero year in Döviken, northern Sweden.
536 *Boreas 14*, 117–122.

537 Cato, I. 1987: On the definitive connection of the Swedish Time Scale with the present.
538 *Sveriges Geologiska Undersökning Ca 68.* 55 pp.

539 Cato, I. 1998: Ragnar Lidén's Postglacial Varve Chronology from the Ångermanälvan
540 Valley, Northern Sweden. *Sveriges Geologiska Undersökning Ca 88.* 82 pp.

541 Cuffey, K.M. & Paterson, W.S.B. 2010: *The physics of glaciers*. 704 pp. Butterworth-
542 Heinemann, Oxford.

543 De Geer, G. 1912: Geochronology of the last 12,000 years. *Proceedings of the*
544 *International Geological Congress 1910*, 241-253.

545 De Geer, G. 1940. Geochronologia Suecica Principles. *Kungliga Svenska*
546 *Vetenskapsakademiens Handligar, Tredje Serien Band 18, No. 6*, 367 pp.

547 Dypvik, H. & Harris, N.B. 2001: Geochemical facies analysis of fine-grained siliciclastics
548 using Th/U, Zr/Rb and (Zr+ Rb)/Sr ratios. *Chemical Geology 181*, 131–146.

549 Gomez, N., Mitrovica, J.X., Huybers, P. & Clark, P.U. 2010: Sea level as a stabilizing
550 factor for marine-ice-sheet grounding lines. *Nature Geoscience 3*, 850–853.

551 Goslar, T., Wohlfarth, B., Björck, S., Possnert, G. & Björck, J. 1999: Variations of
552 atmospheric 14C concentrations over the Alleroød-Younger Dryas transition.
553 *Climate Dynamics 15*, 29–42.

554 Holmquist, B. & Wohlfarth, B. 1998: An evaluation of the Late Weichselian Swedish
555 varve chronology based on cross-correlation analysis. *GFF 120*, 35–46.

556 Johnsen, T.F., Alexanderson, H., Fabel, D. & Freeman, S.P.H.T. 2009: New ^{10}Be
557 cosmogenic ages from the Vimmerby moraine confirm the timing of
558 Scandinavian Ice Sheet deglaciation in southern Sweden. *Geografiska Annaler*
559 *91A*, 113-120.

560 Johnson, M.D., Kylander, M.E., Casserstedt, L., Wiborgh, H. & Björck, S. 2013:
561 Glaciomarine varved clay in central Sweden before and after the Baltic Ice Lake
562 drainage: a further clue to the drainage events at Mt Billingen. *GFF 135*, 293-
563 307.

564 Kristiansson, J. 1986: The ice recession on the southeastern part of Sweden.
565 Stockholm, *University of Stockholm, Department of Quaternary Research, Report*
566 *7*, 133 pp.

567 Lea, J. M., Mair, D. W., Nick, F. M., Rea, B. R., Weidick, A., Kjaer, K. H., Morlighem, M.,
568 Van As, D. & Schofield, J. E. 2014: Terminus-driven retreat of a major southwest
569 Greenland tidewater glacier. *Journal of Glaciology, 60*, 333-344.

570 Lea, J.M., Mair, D.W.F., Nick, F.M., Rea, B.R., As, D.V., Morlighem, M., Nienow, P. &
571 Weidick, A. 2014: Fluctuations of a Greenlandic tidewater glacier driven by
572 changes in atmospheric forcing: observations and modelling of Kangiata
573 Nunaata Sermia, 1859–present. *The Cryosphere, 8*, 2031-2045.

574 Lohne, O.S., Mangerud, J. & Birks, H.H. 2013: Precise 14C ages of the Vedde and
575 Saksunarvatn ashes and the Younger Dryas boundaries from western Norway and
576 their comparison with the Greenland Ice Core (GICC05) chronology. *Journal of*
577 *Quaternary Science 28*, 490–500.

578 Lundqvist, J. 1987: Glaciodynamics of the Younger Dryas marginal zone in Scandinavia.
579 Implications of a revised glaciation model. *Geografiska Annaler 69A*, 305-319.
580
581 Lundqvist, J. & Wohlfarth, B. 2001: Timing and east–west correlation of south Swedish
582 ice marginal lines during the Late Weichselian. *Quaternary Science Reviews 20*,
583 1127–1148.

584 Macleod, A., Brunnberg, L., Wastegård, S., Hang, T. & Matthews, I.P. 2014: Lateglacial
585 cryptotephra detected within clay varves in Östergötland, south-east Sweden.
586 *Journal of Quaternary Science 29*, 605–609.

587 Muscheler, R., Adolphi, F. & Knudsen, M.F. 2014: Assessing the differences between
588 the IntCal and Greenland ice-core time scales for the last 14,000 years via the
589 common cosmogenic radionuclide variations. *Quaternary Science Reviews 106*,
590 81-87.

591 Muschitiello, F. & Wohlfarth, B. 2015: Time-transgressive environmental shifts across
592 Northern Europe at the onset of the Younger Dryas. *Quaternary Science Reviews*
593 *109*, 49–56.

594 Muschitiello, F., Pausata, F.S.R., Watson, J.E., Smittenberg, R.H., Salih, A.A.M., Brooks,
595 S.J., Whitehouse, N.J. Karlatou-Charalampopoulou, A. & Wohlfarth, B. in press:
596 Fennoscandian freshwater control on Greenland hydroclimate shifts at the
597 onset of the Younger Dryas. *Nature Communications.*

598 Nick, F.M., Van der Veen, C.J., Vieli, A. & Benn, D.I. 2010: A physically based calving
599 model applied to marine outlet glaciers and implications for the glacier
600 dynamics. *Journal of Glaciology, 56*, 781-794.

601 Nick, F.M., Vieli, A., Andersen, M.L., Joughin, I., Payne, A., Edwards, T.L. & van de Wal,
602 R.S. 2013: Future sea-level rise from Greenland/'s main outlet glaciers in a
603 warming climate. *Nature, 497*, 235-238.

604 Palmer, A.P., Rose, J., Lowe, J.J. & MacLeod, A. 2010: Annually resolved events of
605 Younger Dryas glaciation in Lochaber (Glen Roy and Glen Spean), Western
606 Scottish Highlands. *Journal of Quaternary Science, 25*, 581-596.

607 Peltier, W.R. 2004: Global glacial isostasy and the surface of the ice-age Earth: the ICE-
608 5G (VM2) model and GRACE. *Annual Reviews of Earth and Planetary Sciences 32*,
609 111–149.

610 Pfahl, S. & Sodemann, H. 2014: What controls deuterium excess in global
611 precipitation? *Climate of the Past 10*, 771–781.

612 Rasmussen, S.O., Andersen, K.K., Svensson, A.M., Steffensen, J.P., Vinther, B.M.,
613 Clausen, H.B., Siggaard-Andersen, M.L., Johnsen, S.J., Larsen, L.B., Dahl-Jensen,
614 D., Bigler, M., Röthlisberger, R., Fischer, H., Goto-Azuma, K., Hansson, M.E. &
615 Ruth, U. 2006: A new Greenland ice core chronology for the last glacial
616 termination. *Journal of Geophysical Research: Atmospheres 111*, D061202.

617 Reimer, P.J., Bard, E., Bayliss, A., Beck, J.W., Blackwell, P.G., Bronk Ramsey, C., Buck,
618 C.E., Cheng, H., Edwards, R.L. & Friedrich, M. 2013: IntCal13 and Marine13
619 radiocarbon age calibration curves 0-50,000 years cal BP. *Radiocarbon 55*,1869-
620 1887.

621 Steffensen, J.P., Andersen, K.K., Bigler, M., Clausen, H.B., Dahl-Jensen, D., Fischer, H.,
622 Goto-Azuma, K., Hansson, M., Johnsen, S.J., Jouzel, J., Masson-Delmotte, V.,
623 Popp, T., Rasmussen, S.O., Rothlisberger, R., Ruth, U., Stauffer, B., Siggaard-
624 Andersen, M.-L., Sveinbjrnsdottir, A.E., Svensson, A. & White, J.W.C. 2008: High-

Resolution Greenland Ice Core Data Show Abrupt Climate Change Happens in Few Years. *Science 321*, 680–684.

Swärd, H., O´Regan, M., Ampel, L., Ananyev, R., Chernykh, D., Flodén, T., Greenwood, S.L., Kylander, M.E., Mörth, C.M., Preto, P. & Jakobsson, M. 2015: Regional deglaciation and postglacial lake development as reflected in a 74 m sedimentary record from Lake Vättern, southern Sweden. *GFF*, 1-19.

Vieli, A., Funk, M. & Blatter, H. 2001: Flow dynamics of tidewater glaciers: a numerical modelling approach. *Journal of Glaciology, 47*, 595-606.

Wohlfarth, B. 1996: The chronology of the last termination: a review of radiocarbon-dated, high-resolution terrestrial stratigraphies. *Quaternary Science Reviews 15*, 267–284.

Wohlfarth, B. & Possnert, G. 2000: AMS radiocarbon measurements from the Swedish varved clays. *Radiocarbon 42*, 323–334.

Wohlfarth, B., Björck, S., Possnert, G., Lemdahl, G., Brunnberg, L., Ising, J., Olsson, S. & Svensson, N.-O. 1993: AMS dating Swedish varved clays of the last glacial/interglacial transition and the potential/difficulties of calibrating Late Weichselian “absolute”chronologies. *Boreas 22*, 113–128.

Wohlfarth, B., Björck, S., Holmqvist, B., Lemdahl, G. & Ising, J. 1994: Ice recession and depositional environment in the Blekinge archipelago of the Baltic Ice Lake. *GFF 116*, 3–12.

Wohlfarth, B., Björck, S. & Possnert, G. 1995: The Swedish time scale; a potential calibration tool for the radiocarbon time scale during the late Weichselian. *Radiocarbon 37*, 347–359.

Wohlfarth, B., Björck, S., Cato, I. & Possnert, G. 1997: A new middle Holocene varve diagram from the river Ångermanälven, northern Sweden: indications for a possible error in the Holocene varve chronology. *Boreas 26*, 347–353.

Wohlfarth, B., Björck, S., Possnert, G. & Holmquist, A.N.D.B. 1998: 800-year long, radiocarbon-dated varve chronology from south-eastern Sweden. *Boreas 27*, 243-258.

Zolitschka, B., Francus, P., Ojala, A.E.K. & Schimmelmann, A. 2015: Varves in lake sediments – a review. *Quaternary Science Reviews 117*, 1–41.

Figure and Table captions

658 **Figure 1.** A. Locations of southern Sweden and NGRIP ice cores. B, C. Location of the
659 sites used to construct the new Lateglacial varve chronology in southern Sweden.
660 Black circles refer to sites studied by Wohlfarth *et al.* (1995). Red circles refer to sites
661 studied by Kristiansson (1986). Blue numbers indicate the sites where the depositional
662 Event 1 (Wohlfarth *et al.* 1998) was identified (see text for details). Note that Event 1
663 can be observed in all the varve diagrams that cover the related time interval. Ice
664 marginal positions are based on Lundqvist & Wohlfarth (2001) and visual
665 interpretation of moraine positions from the LiDAR-based topography. The
666 southernmost ice marginal line refers to the Younger Dryas ice limit (YD). The
667 northernmost ice marginal line refers to the ice limit shortly before the last drainage
668 of the Baltic Ice Lake. Highest shoreline data from Geological Survey of Sweden on a
669 colour scale graded according to present-day elevation (highest lake position was
670 time-transgressive: yellow to red). 1= Bjärka-Säby; 2= Skaggebo; 3= Nåtvin; 4=
671 Vårdnäs; 5= Järnlunden/Stensvassa; 6= Limmern; 7= Storsjön; 8, 9= Mjölsjön; 10=
672 Järnlunden/Sonebo; 11= Bjärsjön; 12, 13, 14= Glottern; 15= Eknäs; 16= Rimforsa; 17=
673 Skedevi; 18= Ytterbo; 19= Räfstad; 20= Äfsinge; 21= Åsunden/Krågedal; 22= Vigerstad;
674 23= Hägerstad; 24= Rävantorpasjön; 25= Lillsjön; 26= Drättinge; 27= Boda; 28=
675 Årteryd; 29= Utdala; 30= Stjärnevik; 31= Tynn/Tyllinge; 32= Tynn/Draboviken; 33=
676 Nedre Emmaren; 34= Bjuggö; 35= Kärra; 36= Lövdalen; 37= Gumhem; 38= Långebro;
677 39, 40, 41= Hargsjön ; 42= Hargsjön 1; 43= Kisa; 44, 45= Adlerskogsjön; 46, 47=
678 Gummetorpasjön ; 48= Kristineberg; 49= Greby; 50= Åby; 51= Väsby; 52= Dråpetorp;
679 53= Brunebo; 54= Järpekullen; 55= Kåreda. The location of Gropviken and Sandfjärden
680 is also shown (green circles). LiDAR topography © Lantmäteriet.
681

682 **Figure 2.** Length of the varve-thickness diagrams used to construct the chronology
683 presented in Wohlfarth *et al.* (1998) and displayed on the local varve time scale
684 proposed by Kristiansson (1986). The chronology is based on diagrams studied by
685 Kristiansson (1986) and Wohlfarth *et al.* (1995), which were visually and statistically
686 cross-correlated with each other (Holmqvist & Wohlfarth 1998). Numbers refer to the
687 original coding scheme used by Holmqvist & Wohlfarth (1998). The three major
688 depositional events identified by Wohlfarth *et al.* (1998) are also shown at the bottom.
689 The events are characterised by distinct colour changes of the clay varves and a
690 marked drop in varve thickness that last for a few decades (see text for details).
691
692 **Figure 3.** Varve-width and stratigraphic alignment of the varve records forming the
693 new composite Lateglacial varve chronology from Småland/Östergötland presented
694 on the local varve time scale (Kristiansson 1986). The two northernmost successions
695 of Gropviken and Sandfjärden were first cross-correlated with each other. Prior to
696 cross-correlation time series were detrended applying a 16^{th} degree Fourier
697 transform, filtered using a 3-year moving average and removing the first 10 bottom
698 varves, and normalized by their standard deviation. The correlation coefficient (*r*) and
699 statistics (signal-to-noise ratio *z* and *p*-value) between the individual records are given
700 in the graph. Sandfjärden's chronology was correlated to the 806-year long master
701 chronology (Wohlfarth *et al.* 1998) via common stratigraphic markers (two marked
702 colour changes and an exceptionally thick varve layer). The master chronology
703 presented here was filtered by removing the first 10 bottom varves of each varve
704 diagram.
705

706 **Figure 4.** Top panel: Wiggle-matching age model of the Lateglacial varve chronology
707 (LGC) and verification of its placement relative to the chronology of Gropviken
708 containing the Vedde Ash time marker. The age model of the LGC is based on
709 radiocarbon dates from selected terrestrial plant macrofossils previously published in
710 Wohlfarth *et al.* (1998) (blue crosses; Table 1). A radiocarbon-based calendar age for
711 the Vedde Ash in Gropviken (red cross) was assigned using precise estimates from
712 Lake Kråkenes in Western Norway (Lohne *et al.* 2013). The most likely position of each
713 radiocarbon estimate on the modelled IntCal13 calibration curve (grey; Reimer *et al.*
714 2013) is shown. In the upper-left panel is presented the comparison of the estimated
715 offsets between the LGC and Gropviken using cross-correlation and radiocarbon-
716 based methods, respectively (see text for details). The goodness of the placement of
717 the LGC relative to Gropviken is further confirmed by the position of the Allerød-
718 Younger Dryas pollen-defined boundary on the master chronology, which is consistent
719 with previously reported age estimates for this biostratigraphic event (Muschitiello &
720 Wohlfarth 2015). The probability distribution functions of the most likely placement
721 on the IntCal13 time scale of the LGC and the Vedde Ash, respectively, are also shown
722 together with their 2 sigma standard error. Bottom panel: Plot showing varve-age
723 against depth (blue dots and dashed line). The varve-age-depth relationship is
724 compared to the calibrated ^{14}C curve based on the unmodelled radiocarbon
725 measurements listed in Table 1 (black dots). Bars indicate 2 sigma standard error
726 associated with each measurement and the additional varve-age error related to
727 macrofossil sampling (Wohlfarth *et al.* 1998). The varve-age scale is based on
728 synchronization to the IntCal13 time scale using the radiocarbon-based age estimate
729 of the Vedde Ash (red dot).

730

731 **Figure 5.** The new Lateglacial varve chronology presented as a unified record of mean
732 varve thickness and plotted against the GICC05 time scale (after converting the b2k
733 age into BP) and IntCal13 time scale after synchronization via the Vedde Ash isochron
734 and wiggle-match modelling, respectively. Mean annual varve widths are displayed
735 together with a 10-year running average (red line). The chronology is plotted with a
736 record of ice-rafted mineral debris (blue histogram) formerly published in Wohlfarth
737 *et al.* (1998). The vertical dashed lines indicate the interval analysed for ice-rafted
738 debris grains. The three major depositional events identified by Wohlfarth *et al.* (1998)
739 are also displayed. The green bar shows the timing of the regional AL-YD pollen
740 boundary as defined in the Lateglacial varve chronology (Björck, 1999), which lags the
741 onset of Greenland Stadial 1 by ~150 years.

742

743 **Figure 6.** XRF elemental results from new Gummetorpasjön's varve records. All data
744 are smoothed using a 10-point running mean to facilitate visualization (black line). For
745 reference, the XRF data are presented with the optical and radiographic
746 stratigraphies. The stratigraphic transition referred to as Event 1 and synchronous
747 with the start of Greenland Stadial 1 in ice-core records is highlighted by the red
748 dashed line. The XRF elemental profiles consistently show relative changes in ratio
749 values 18-19 varve years before Event 1 (shaded area). Note inverse axis for Zr/Rb
750 ratios.

751

752 **Figure 7.** Results of idealised model runs showing change in calving fluxes and
753 terminus position 10 years after an instantaneous drop in lake level is applied. These

754 are shown for three different initial lake levels, and three different potential lake level
755 drops. These experiments were run for (A) low, (B) medium, and (C) high basal
756 roughness scenarios.
757
758 **Figure 8.** Calendar age of Event 1 in the new Lateglacial varve chronology relative to
759 the GICC05 and IntCal13 time scale and compared with estimated age of the start of
760 Greenland Stadial 1 in Greenland ice cores. The age of Event 1 is also compared with
761 the combined probability of a number of calibrated radiocarbon dates constraining
762 the timing of the first drainage of the Baltic Ice Lake and presented in Muschitiello *et*
763 *al.* (in press). The calibrated radiocarbon dates refer to lake isolations from the sea,
764 which indicate timing of deglaciation of the outlet system west of Mount Billingen in
765 southern Sweden, near 11 000 ^{14}C years BP (Björck and Digerfledt 1982a, b). Two dates
766 refer to isolation owing to concomitant lowering of the Baltic Ice Lake in Blekinge
767 (Björck 1979) and one refers to the timing of the Baltic Ice Lake water-level fall as
768 recorded in Arkona Basin, southern Baltic Sea (Bennike & Jensen 2013). All ages are
769 here presented with their 1 sigma uncertainty and error bars. Under the assumption
770 of synchronicity between Event 1, the first drainage of the Baltic Ice Lake and the onset
771 of Greenland Stadial 1, the estimated offset between the GICC05 (after converting the
772 b2k age into BP) and the IntCal13 time scales at the transition into Greenland Stadial
773 1 is of 30±22 years (1σ).
774
775 **Table 1.** AMS ^{14}C dates from glacilacustrine varves of the Östergötland master
776 chronology. All dates are based on selected terrestrial plant remains and used to
777 construct the Bayesian wiggle-matching age model presented in this study.

778

779 **Table 2.** Input parameters used in the ice flow/calving model experiments.

780 Table **Error! No sequence specified.**

Sample ID	Site	Local Varve Years	^{14}C age (year)	^{14}C error (1 sigma)	Used in the age model
Ua-11233	Nedre Emmaren	2221±52	10 740	240	No
Ua-10181	Gummetorpasjön	2199±32	11 450	240	No
Ua-11234	Nedre Emmaren	2146±23	10 885	250	Yes
Ua-3131	Tynn	2125±35	10 890	120	Yes
Ua-10182	Gummetorpasjön	2123±30	11 470	130	No
Ua-10183	Gummetorpasjön	2090±18	11 030	120	Yes
Ua-4358	Hargsjön	2055±50	10 980	100	Yes
Ua-10184	Gummetorpasjön	2044±16	10 970	90	Yes
Ua-2753	Hargsjön	2010±45	10 480	150	No
Ua-10185	Gummetorpasjön	2009±16	11 230	100	No
Ua-4493	Adlerskogssjön	2003±59	10 830	165	Yes
Ua-4359	Hargsjön	1973±31	10 610	110	Yes
Ua-10186	Gummetorpasjön	1968±25	11 040	110	No
Ua-10187	Gummetorpasjön	1938±4	10 420	220	Yes
Ua-4496	Glottern	1856±50	10 585	465	No

781
782
783

Table 2

Parameter/Constant	Value
Ice density – ρ_i	900 kg m^{-3}
Meltwater density – ρ_w	1000 kg m^{-3}
Proglacial water body density – ρ_p	1000 kg m^{-3}
Gravitational acceleration - g	9.8 m s^{-2}
Friction exponent - m	3
Excess floatation fraction - q	0.09
Glen's flow law exponent - n	3
Glen's flow law coefficient - A	2.93 x 10^{-17} Pa^{-3} a^{-1}
	Corresponding to -5 °C (Cuffey & Paterson, 2010)
Initial grid size	~250 m
Time step	0.005 a

784
785

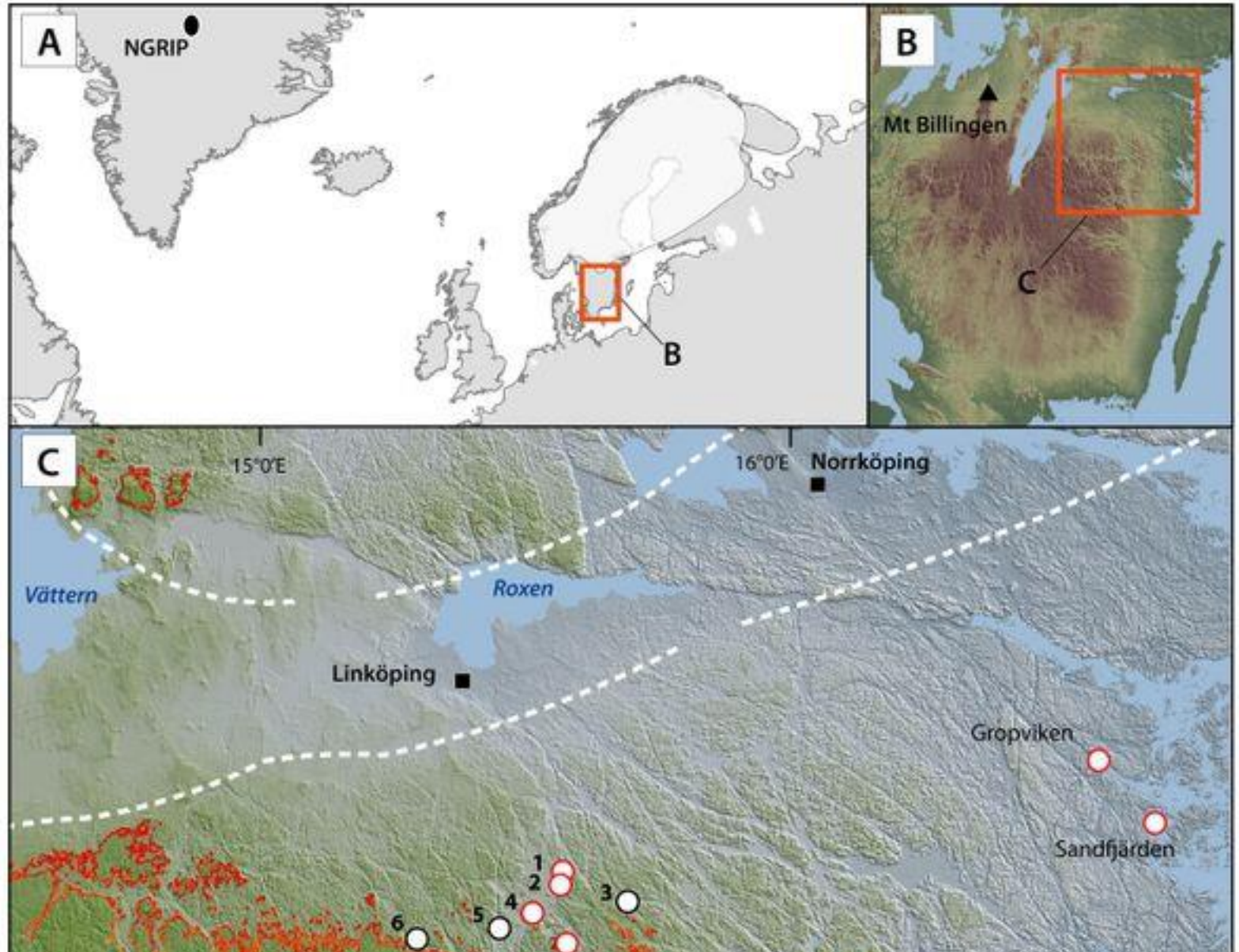
A
NGRIP
B
B
Mt Billingen
C
C
15°0'E
16°0'E
Norrköping
Vättern
Roxen
Linköping
Gropviken
Sandfjärden
1
2
3
4
5
6

Fig

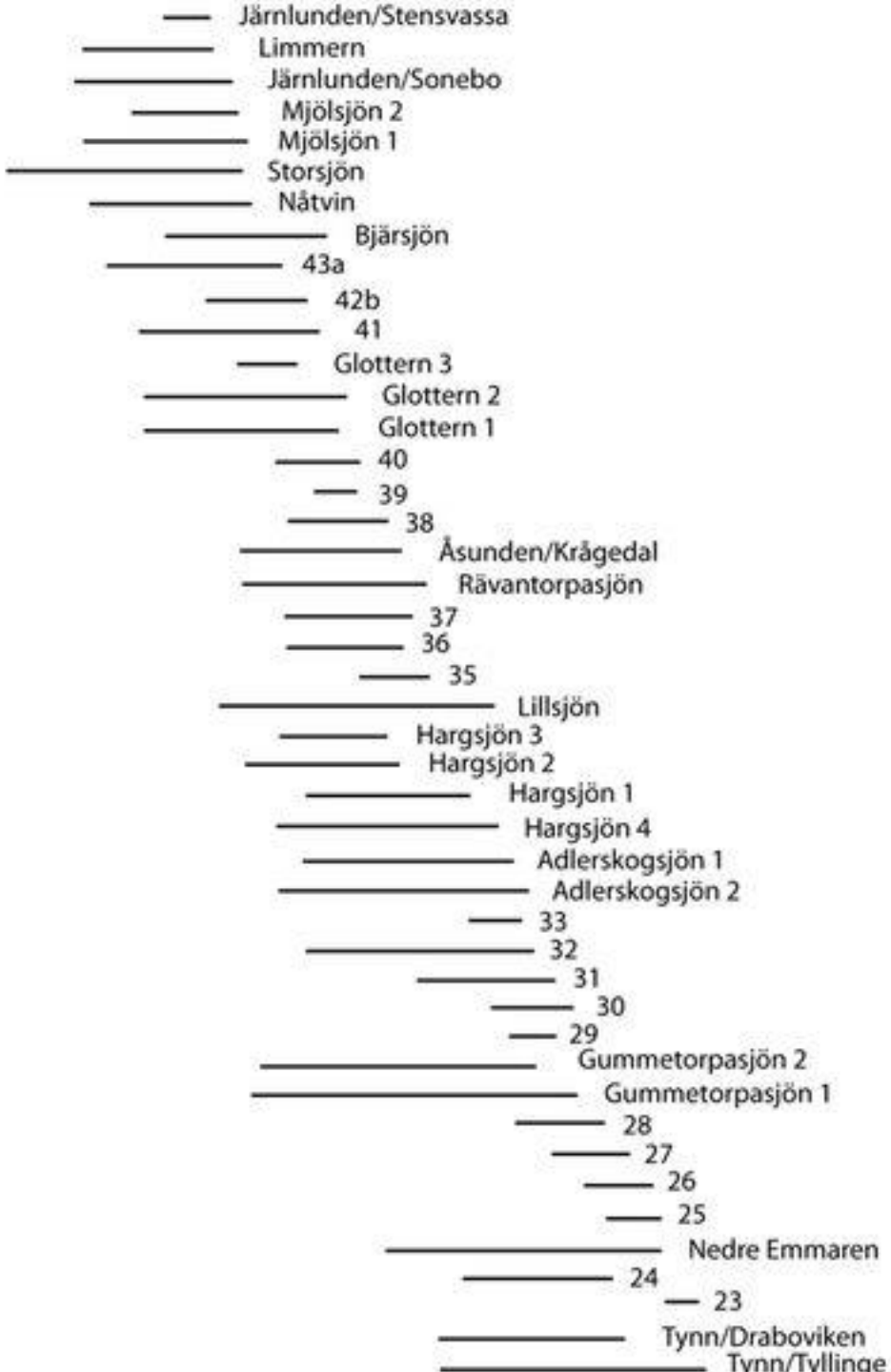
Järnlunden/Stensvassa
Limmern
Järnlunden/Sonebo
Mjölsjön 2
Mjölsjön 1
Storsjön
Nåtvin
Bjärsjön
43a
42b
41
Glottern 3
Glottern 2
Glottern 1
40
39
38
Åsunden/Krågedal
Rävantorpasjön
37
36
35
Lillsjön
Hargsjön 3
Hargsjön 2
Hargsjön 1
Hargsjön 4
Adlerskogsjön 1
Adlerskogsjön 2
33
32
31
30
29
Gummetorpasjön 2
Gummetorpasjön 1
28
27
26
25
Nedre Emmaren
24
23
Tynn/Draboviken
Tynn/Tyllinge

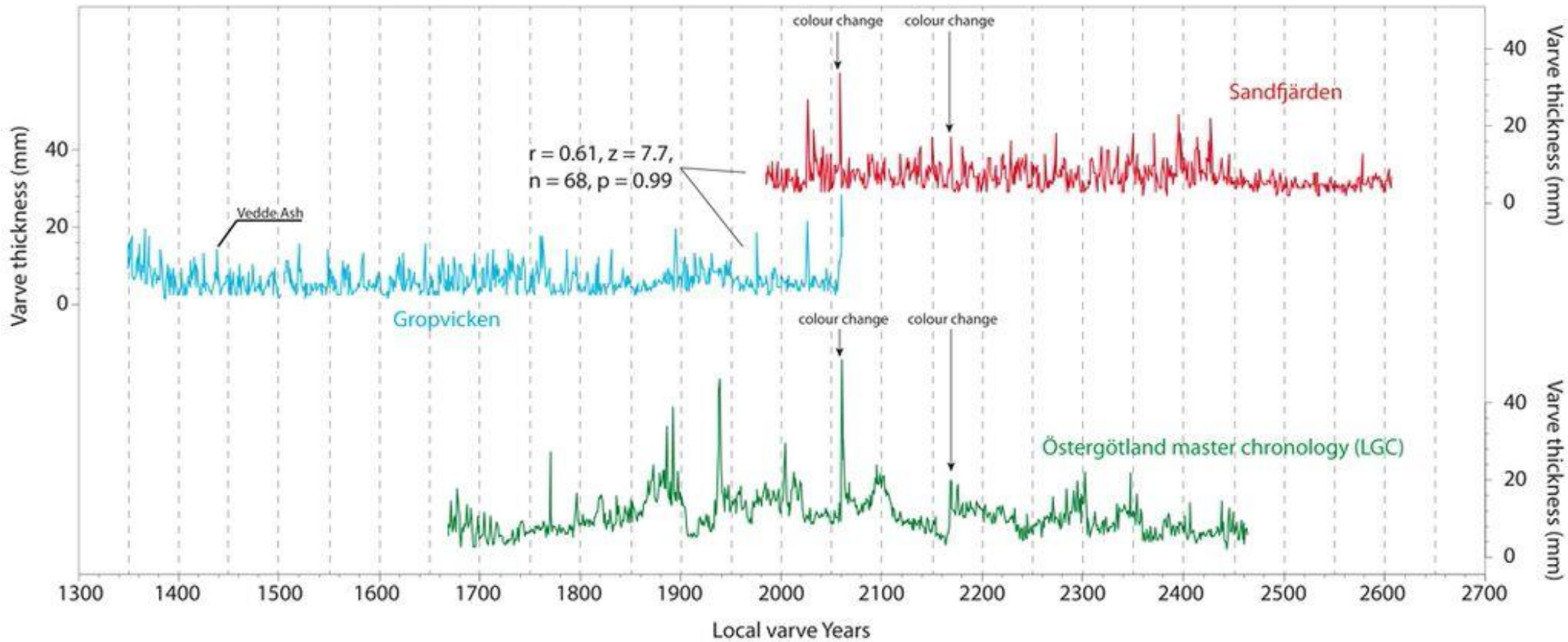
colour change
colour change
Sandfjärden
r = 0.61, z = 7.7,
n = 68, p = 0.99
Vedde Ash
Gropvicken
colour change
colour change
Östergötland master chronology (LGC)
Varve thickness (mm)
Varve thickness (mm)
Varve thickness (mm)
0
20
40
1300
1400
1500
1600
1700
1800
1900
2000
2100
2200
2300
2400
2500
2600
2700
Local varve Years

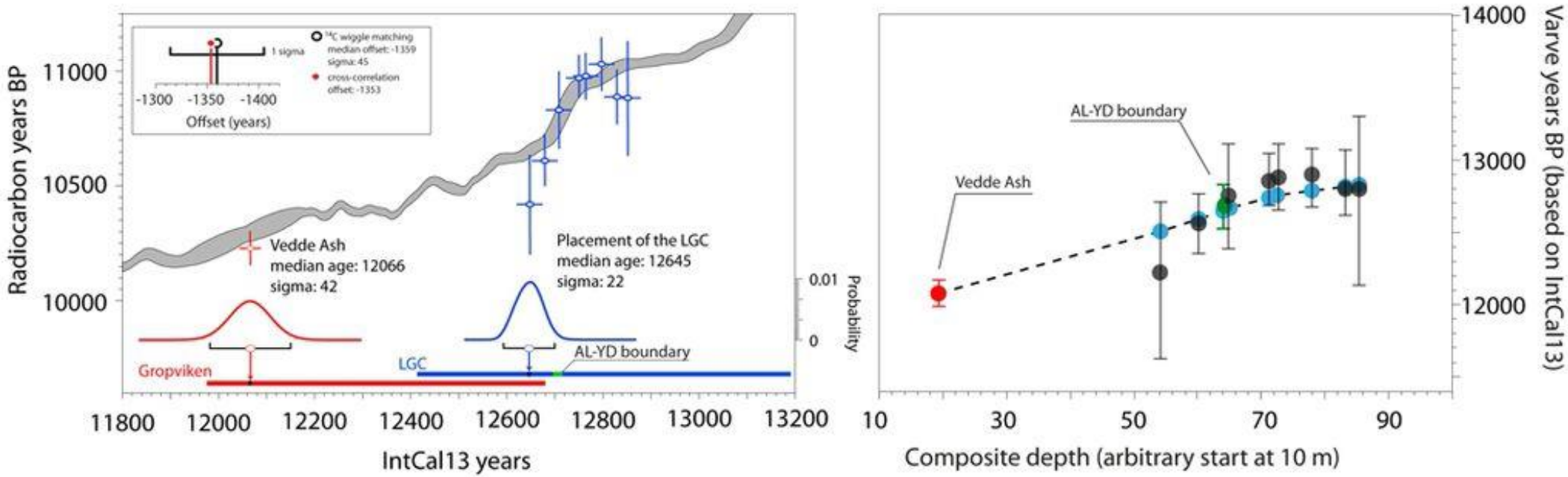
Radiocarbon years BP
11000
10500
10000
11800
12000
12200
12400
12600
12800
13000
13200
IntCal13 years
1 sigma
-1300
-1350
-1400
Offset (years)
14C wiggle matching
median offset: -1359
sigma: 45
cross-correlation
offset: -1353
Vedde Ash
median age: 12066
sigma: 42
Placement of the LGC
median age: 12645
sigma: 22
0.01
0
Probability
Gropviken
LGC
AL-YD boundary
AL-YD boundary
Vedde Ash
14000
13000
12000
Varve years BP (based on IntCal13)
10
30
50
70
90
Composite depth (arbitrary start at 10 m)

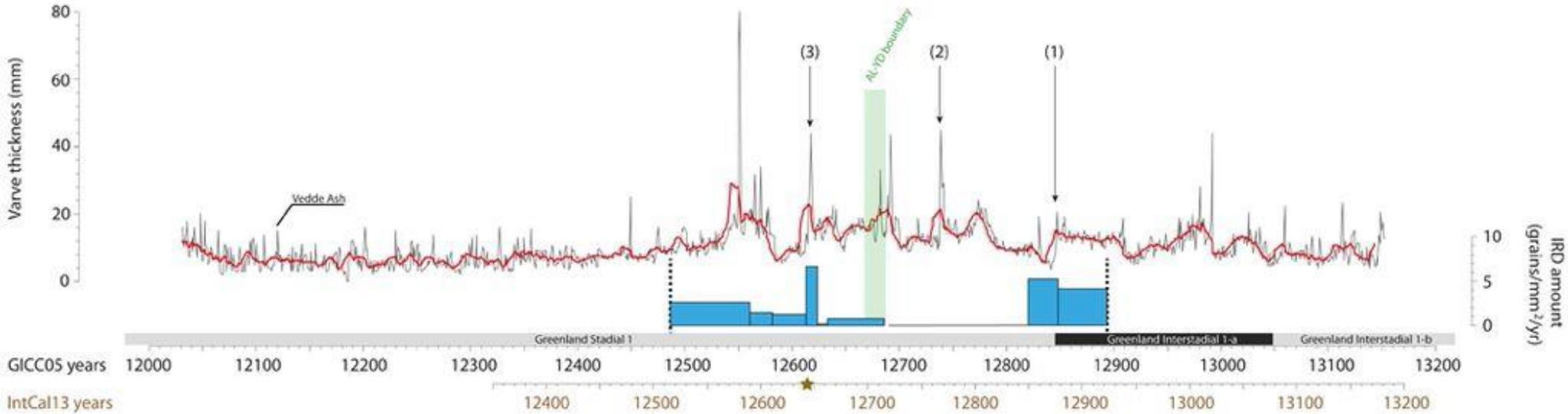
Varve thickness (mm)
80
60
40
20
0
Vedde Ash
(3)
(2)
(1)
AL-YD boundary
IRD amount (grains/mm²/yr)
10
5
0
Greenland Stadial 1
Greenland Interstadial 1-a
Greenland Interstadial 1-b
GICC05 years
12000
12100
12200
12300
12400
12500
12600
12700
12800
12900
13000
13100
13200
IntCal13 years
12400
12500
12600
12700
12800
12900
13000
13100
13200

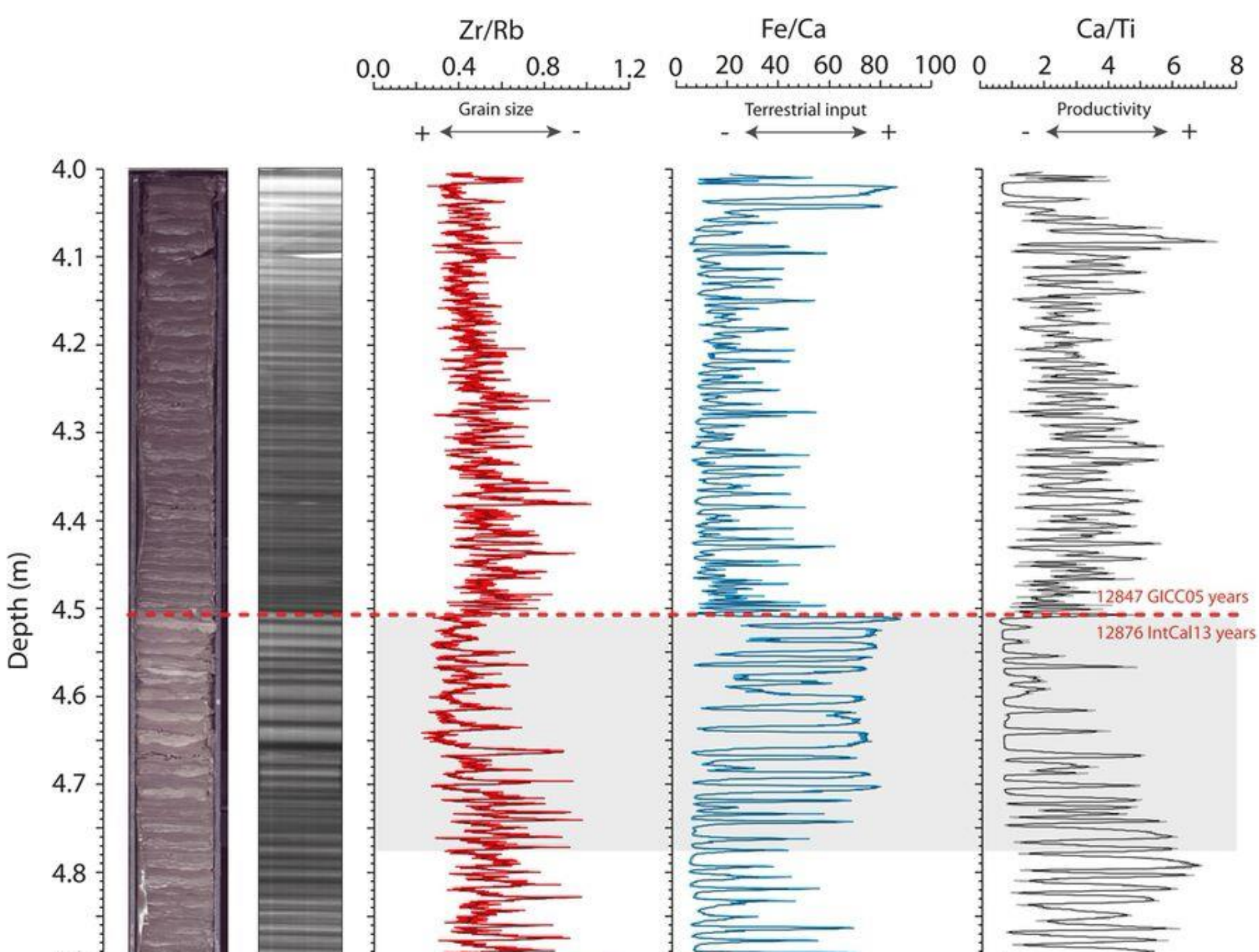
Zr/Rb
0.0
0.4
0.8
1.2
Grain size
+
-
Fe/Ca
0
20
40
60
80
100
Terrestrial input
-
+
Ca/Ti
0
2
4
6
8
Productivity
-
+
Depth (m)
4.0
4.1
4.2
4.3
4.4
4.5
4.6
4.7
4.8
12847 GICC05 years
12876 IntCal13 years

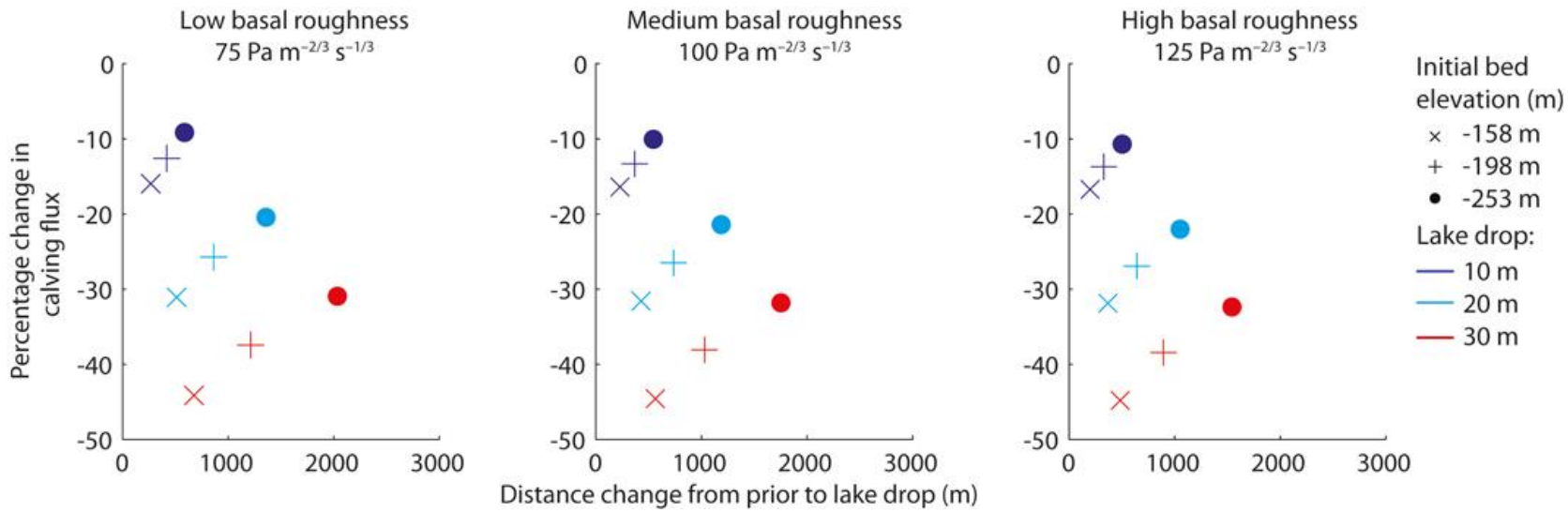
Low basal roughness
75 Pa m$^{-2/3}$ s$^{-1/3}$
Medium basal roughness
100 Pa m$^{-2/3}$ s$^{-1/3}$
High basal roughness
125 Pa m$^{-2/3}$ s$^{-1/3}$
Percentage change in calving flux
0
-10
-20
-30
-40
-50
0
1000
2000
3000
Distance change from prior to lake drop (m)
Initial bed elevation (m)
-158 m
-198 m
-253 m
Lake drop:
10 m
20 m
30 m

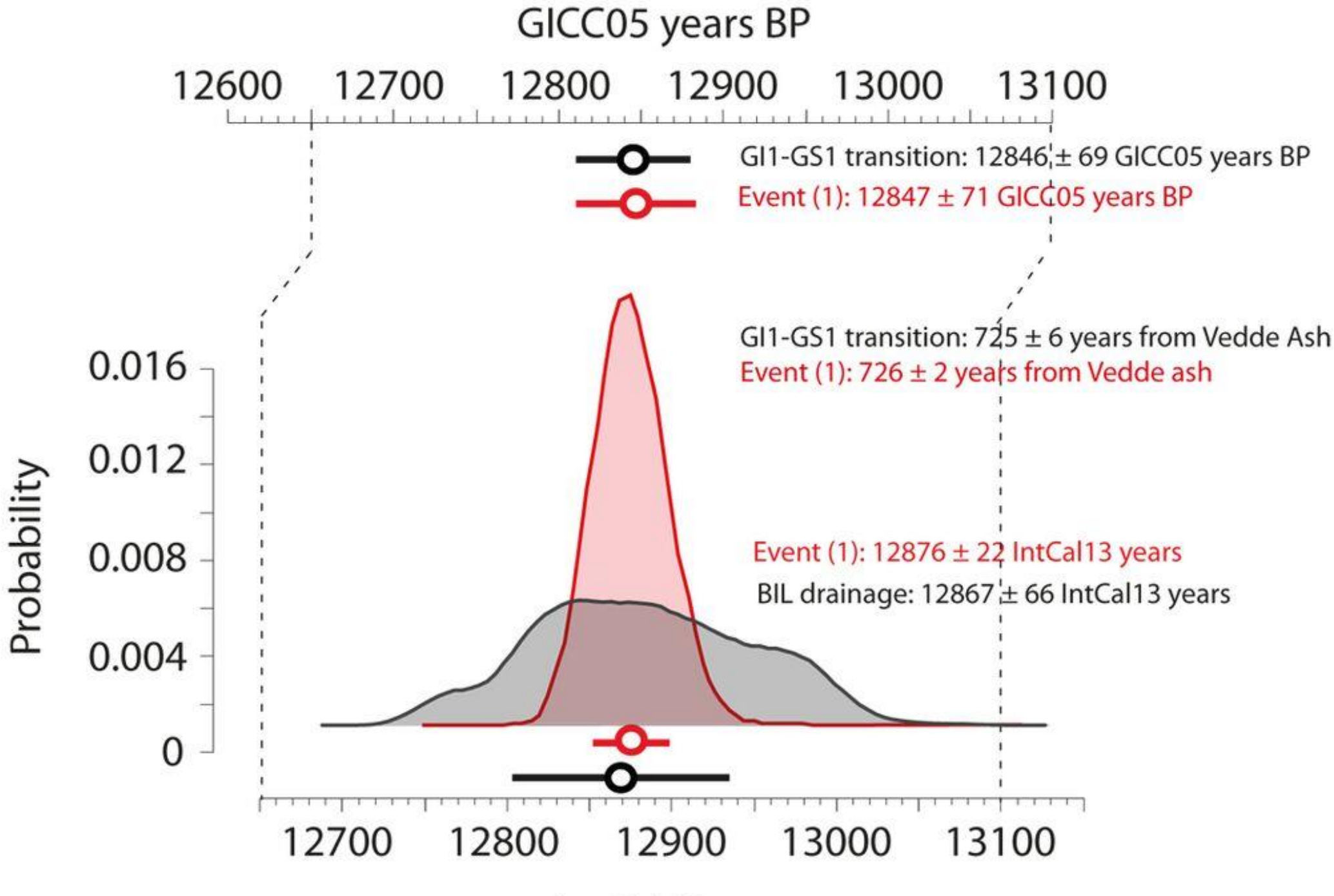
GICC05 years BP
12600
12700
12800
12900
13000
13100
GI1-GS1 transition: 12846 ± 69 GICC05 years BP
Event (1): 12847 ± 71 GICC05 years BP
GI1-GS1 transition: 725 ± 6 years from Vedde Ash
Event (1): 726 ± 2 years from Vedde ash
Event (1): 12876 ± 22 IntCal13 years
BIL drainage: 12867 ± 66 IntCal13 years
Probability
0.016
0.012
0.008
0.004
0
12700
12800
12900
13000
13100